

Harmonic Elimination Using a Novel Optimization Algorithm in a Multilevel Inverter

B Thejasvi¹, Dr. P. Vijayapriya^{2*}

^{1,2*}Vellore Institute of Technology, Vellore, Tamilnadu. India

Email: ¹tejasvibathyala@gmail.com ^{2*}pvijayapriya@vit.ac.in

Corresponding Author: Dr. P. Vijayapriya

Abstract

This research describes a seven-level RSS-MLI, a reduced switch symmetrical multilevel inverter employs MPPT or maximum power point tracking, is determined by perturbation and observation (P&O) for photovoltaic (PV) power generation. Using the MPPT technology, solar PV cells may produce their maximum power output. By utilizing solar radiation and PV cell temperature as input factors, the method establishes the ideal duty cycle in order to guarantee the greatest output regarding DC-DC boost converter. The Proportional Integral Derivative of Fractional Order (FOPID) optimized using SBOA or Secretary Bird Optimization Algorithm is the basis for the method of Selective Harmonic Elimination (SHE) approach utilized by RSS-MLI to eliminate harmonics from the output voltage. Inspired by secretary bird survival behaviour in the wild, SBOA is a metaheuristic algorithm that is based on populations. The SBOA is utilized for optimizing the FOPID controller for selecting the optimum duty cycle of the RSS-MLI for the total harmonic distortion (THD) reduction. Performances are assessed using the proposed method in MATLAB/Simulink implementation and contrasted with traditional methods such as GA-PID, Controllers for WSOA-PID and WSOA-FOPID.

Keywords: PV array, load, SBOA, RSS-MLI, MPPT, THD, and FOPID controller

1) Introduction

Renewable energy sources have become a significant substitute for traditional energy sources in recent years [1]. PV cell energy stands out among renewable energy sources due to its reduced carbon emissions and minimal maintenance requirements [2]. the reason a boost converter from DC to DC is utilized is because its voltage output is significantly lower than the majority of other networks voltage rating [3]. Consequently, to generate the highest voltage from the PV array by utilizing a boost converter, an MPPT control method is applied. [4].

¹ Abdalla, OH, et al., University of Khartoum Engineering Journal, vol. 09, no. 02, pp. 18-24.

² Ali, I, Sharma, V et al., International Journal on Future Revolution in Computer Science & Communication Engineering, vol. 04, no. 01, pp. 5-11.

³ Bihari, SP et al., Analog Integrated Circuits and Signal Processing, pp. 1-14.

⁴ Castillo, et al., IET Power Electronics, vol. 11, no. 04, pp. 700-707.

Several MPPT control strategies have been utilized recently. Because of its ease of use and simplicity, MPPT controllers frequently use the P&O approach [5]. Since most loads are AC loads, commercial applications need for the higher output voltage will be converted to AC using the DC-DC boost converter [6].

During the inversion phase, conventional three-level inverters are frequently utilized; however, their efficiency is constrained, and they suffer from excessive voltage stress and electromagnetic interference [7]. In this regard, multilayer inverters, or MLIs, are becoming increasingly popular in both commercial and small- to large-scale industries [8]. The MLI's remarkable harmonic profile and ability to function at both high switching and fundamental switching frequencies make it an appealing feature [9]. In the literature, several MLI topologies, including diode clamped, flying capacitor, and CHB-MLI, have been introduced and examined for DC to AC conversion [10]. Due to the need for voltage balancing, a flying capacitor inverter requires more capacitors than a diode clamped (neutral point) inverter, which requires more diodes [11]. However, output voltage of the CHB-MLI produces fewer harmonic components. The voltage output quality of CHB-MLI is gradually improved by expanding the number of output levels available [12]. CHB-MLIs are more suited for PV array applications because they allow a single module will house all of the H-bridge cells and give each PV panel its own independent DC voltage source [13].

⁵ Deepak, K, et al., *Innovations in Electrical and Electronics Engineering*, Springer, pp. 203-213.

⁶ Gaur, P, Verma, YP et al., *Advances in Electrical Control and Signal Systems*, Springer, pp. 541-551.

⁷ Humayun, M, et al., *International Journal of Electrical Power & Energy Systems*, vol. 115, pp. 105430.

⁸ Katoch, S., et al., *Multimed Tools Application*, vol. 80, pp. 8091-8102.

⁹ Kiran Kumar, G, et al., *Energies*, vol. 13, no. 06, pp. 1299-1310.

¹⁰ Kumar, J, et al., *International Journal of Engineering Research & Technology (IJERT)*, vol.9, no.1, pp.208-214.

¹¹ Masoudinia, F, et al., *International Journal of Electronics*, pp. 1-18.

¹² Premkumar, M, Sumithira, T et al., *International Journal of Intelligent Engineering and Systems*, vol. 11, no. 02, pp. 18-27.

¹³ Robinson, P et al., *International Journal of Pure and Applied Mathematics*, vol. 118, no. 16, pp. 999-1013.

The quantity of switches in an MLI determines its size, cost, complexity, and reliability. Therefore, the ratio of the required voltage level to the required number of switches is the crucial component in constructing MLI [14]. A unique circuit architecture that uses fewer switches and no extra H-bridges has been created to generate the identical output to that of a seven-level CHB MLI [15]. This study also informs on the progress made on the 7-level MLI design with decreased switches based on PV. In comparison to CHB MLI, this architecture produces the same voltage output with fewer switches, fewer devices, and lower costs.

The literature has offered several sophisticated control strategies for adjusting the MLI with the goal of lowering the THD [16]. They can be separated into two categories as low and high switching frequency control techniques. The techniques are minimizing switching frequency, particularly the THD; to a low value are widely used [17]. However, the main issue with these strategies is increased switching loss, which is why low/fundamental switching frequency control techniques are better in this regard [18]. SHE is a well-known fundamental switching control system that can significantly minimize the THD by eliminating the intended dominating lower order harmonics. The SHE method requires a collection of problem's solution trigonometric Fourier series transcendental equations to determine the precise switching angles [19]. By approaching it as an optimization problem rather than an algebraic numerical problem, this issue can be avoided. Several optimization approaches are used to ascertain the best angles for switching, Includes colonial competitive algorithm (CCA), the firefly algorithm (FA), genetic algorithm (GA), and particle swarm optimization (PSO) [20]. This algorithm's primary issues are its lack of memory and sluggish rate of convergence, which caused it to become stuck at some local minima when solving a multi-optimal problem. The SBOA approach can be hybridized with a FOPID controller to address these issues.

¹⁴ Sadu, S, et al., Iranian Journal of Electrical and Electronic Engineering, vol. 14, no. 01, pp. 95-105.

¹⁵ Salem, A, et al., IEEE Journal on Emerging and Selected Topics in Circuits and Systems, vol. 05, no. 03, pp. 430-442.

¹⁶ Sarika D Patil et al.,Hybrid Optimization Algorithm Applied for Selective Harmonic Elimination in Multilevel Inverter with Reduced Switch Topology.

¹⁷ Shunmugham Vanaja, D et al., International Transactions on Electrical Energy Systems, vol. 30, no. 04, pp. 122-127.

¹⁸ Siddique, et al.,International Transactions on Electrical Energy Systems, vol. 30, no. 02, pp.12191- 12198.

¹⁹ Sim, S, et al., 'Enhance Cascaded H-Bridge Multilevel Inverter with Artificial Intelligence Control', Indonesian Journal of Electrical Engineering and Computer Science,

²⁰ Thiruvengadam, A et al.,Conduction, and Switching Losses Using Sinusoidal Tracking Algorithm', Energies, vol. 12, no. 01, pp. 1-22.

2) Recent research works: An overview

For renewable energy applications, different topologies of symmetric and asymmetric multilevel inverters with fewer switches have been investigated recently. This section reviews a limited number of recent works.

Rohit Kumar and Bhim Singh [21] have presented an asymmetric hybrid inverter for a medium voltage drive with lower power components. A structure was designed with a series connection of (1:1) dc-source-based level generator unit with polarity converter H-bridge, which was cascaded to a conventional H-bridge, whose dc source magnitude was double. An eleven-step inverter was set up with three DC sources and 10 power switches. An extension of inverter to higher voltage levels could easily be achieved by cascading several level-generator and H-bridge units. Most of the power switches were turned on and off at a low and fundamental frequency because of the use of the SHE, which greatly lowers losses and increases converter efficiency. The SHE also has the advantage of precisely controlling the harmonic spectrum produced by a specific voltage and/or current waveform by a power converter. Using PSO, the nonlinear equation of the selected harmonic was optimally solved.

The multilevel converters (MLCs) performance is subject to the unpredictability of DC sources have proposed by Omid Zolfagharian et al. [22]. Because of their more separated dc sources, three-phase cascaded H-bridge (CHB) MLCs are more negatively impacted by this problem. While DC voltage variation can occur in any phase, the impact of one phase online voltage change was examined. To address these issues and improve line voltage resistance to dc voltage changes while also mitigating third harmonic, the quarter-wave symmetrical SHE formulation for three-phase CHB-MLCs must be modified. Non-identical modulation indices must be used to fully use the potential of dc voltages to maintain stable line voltage amplitude when dc voltages change. Furthermore, a technique depending on each phase's average dc voltage (ADCV) was incorporated in the formulation of the SHE to mitigate uneven dc voltages that may arise in several states within a phase.

Mehmet Halil Yabalar and Ergun Ercelebi [23] have introduced a hybrid optimization strategy that blends the optimization-centric on teaching and the learning (TLBO) and the whale optimization algorithm (WOA) for SHE technique in a modified reduced switch topology three phase MLI. The topology requires fewer switches than a conventional cascaded H-bridge MLI and another reduced switch topology in a single phase MLI.

²¹ Rohit Kumar et al., "Reduced Power Components Based Asymmetric Multilevel Inverter with Elimination of Lower Order Harmonics.

²² Omid Zolfagharian, et al., IEEE Journal of Emerging and Selected Topics in Power Electronics.

²³ Mehmet Halil Yabalar et al., IEEE Access, vol. 12, pp. 71010-71023, 2024

Once applied to an 11-level inverter, the hybrid strategy effectively tackles the issues of harmonic reduction and THD on the line-to-line voltage, enhancing output power's quality considerably by the optimal determination of switching angles. The non-linear set of equations related to the SHE controls approach is solved by using the TLBO and WOA, aiming to overcome the limitations of classical methods prone to local optimal solutions and dependent on initial controlling parameters. This method has been performed in two steps, during the first step TLBO has been executed and in the next step the solutions derived from TLBO has been used as an initial guess for WOA which ensures the attainment of the precisely converged solution.

Niraimathi Ramachandran et al., [24] have showed a 21-level cascaded asymmetric inverter with a reduced switch count. The system uses a solar photo voltaic (SPV) source and a battery as well. The topology of the 21-level inverter needs 3 three power supplies with voltages in the ratio 1:2:7. The two lower voltage levels in the ratio V and $2V$ are connected in series. In contrast, the third one, which is in the $7V$ level, is isolated. The proposed idea uses a step modulation strategy. The step angles are selected strategically by fixing the switching angles at predetermined values.

V.Kubendran et al. [25] have described a double source double diode double switch (DSDDDS) MLI for generating a connected polarity-changing circuit of an H-bridge inverter for the purpose of producing negative voltage and positive voltage. The number of fundamental components is connected to reach the required level. With fewer switches, more stepped levels may be made, a variety of algorithms are provided, including two newly devised algorithms and variations on the sequences that are Binary, Natural, Quasi-Linear and Trinary.

3) Proposed methodology

The proposed system contains PV, P&O MPPT controller, DC-DC converter, RS-MLI and SBOA optimized FOPID controller for managing THD of the load output. The design of the suggested system is shown in Figure 1. Both DC and AC loads are controllable. To meet the demands of the load in the suggested configuration, the system generates energy using photovoltaic cells. The purpose of RS-MLI is to convert a significant quantity of DC to AC output levels with fewer switching components and at a cheap price. The switches' need for voltage is decreased by the suggested RS-MLI circuit while improving consideration of deviation failure and protection against overvoltage.

²⁴ Niraimathi Ramachandran, et al., A Novel 21-Level Asymmetric Multilevel Inverter with Reduced Switches for Solar PV Systems, *Electric Power Components and Systems*, pp.1–20, 2024

²⁵ V.Kubendran, et al., "The development of a generalized multilevel inverter for symmetrical and asymmetrical dc sources with a minimized-ON state switch", *Ain Shams Engineering Journal*, Vol.15, No.2, 102358, pp.1-10, 2024

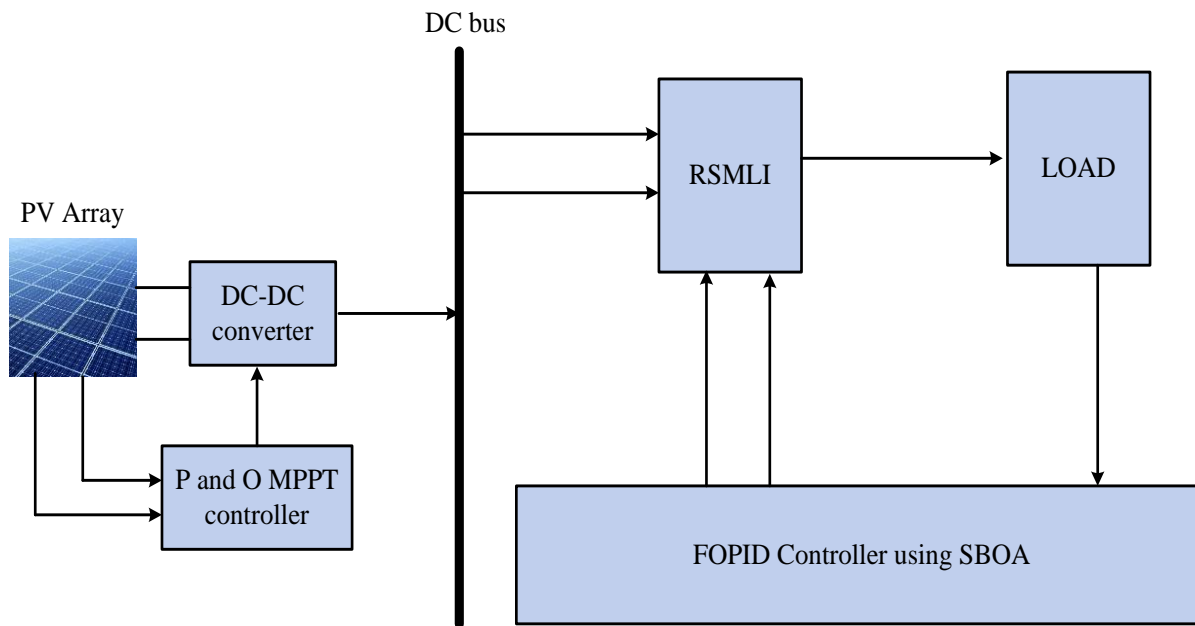


Figure.1: The suggested SBOA optimized FOPID controller's architecture

The purpose DC-DC converters are used to boost the PV energy, and adding a P&O MPPT controller can boost the power from photovoltaic sources in a variety of environmental circumstances. The suggested structure uses both linear and nonlinear loads to regulate power. By optimizing the gain parameter using the SBOA, the suggested FOPID controller improves the load power parameters.

3.1) Modelling of Photovoltaic Solar Cell

Utilizing renewable energy sources is advantageous for a number of reasons, including the fact that they don't make noise, require maintenance, or produce pollution. Semiconductor-based PV cells convert solar light into electrical energy by means of the photovoltaic effect. These days, PV arrays are often utilized in independent or grid-connected applications. The following is the definition of the optimal PV cell equation for producing the I–V characteristic.

$$I = I_{PV} - I_D \tag{1}$$

$$I_D = I_0 \left[\exp\left(\frac{cV}{\alpha KT}\right) - 1 \right] \tag{2}$$

Here, the reverse saturation current I_0 and I_{PV} the current produced by the solar cell. The Shockley diode equation shows as I_D . The electron charge ($1.60217646 \times 10^{-19} C$) stand for c ,

the diode ideality factor constant is α , K is the Boltzmann constant ($1.3806503 \times 10^{-23} \text{ J/K}$), and the absolute temperature T . Figure 2 depicts the single diode structure of a comparable PV cell circuit.

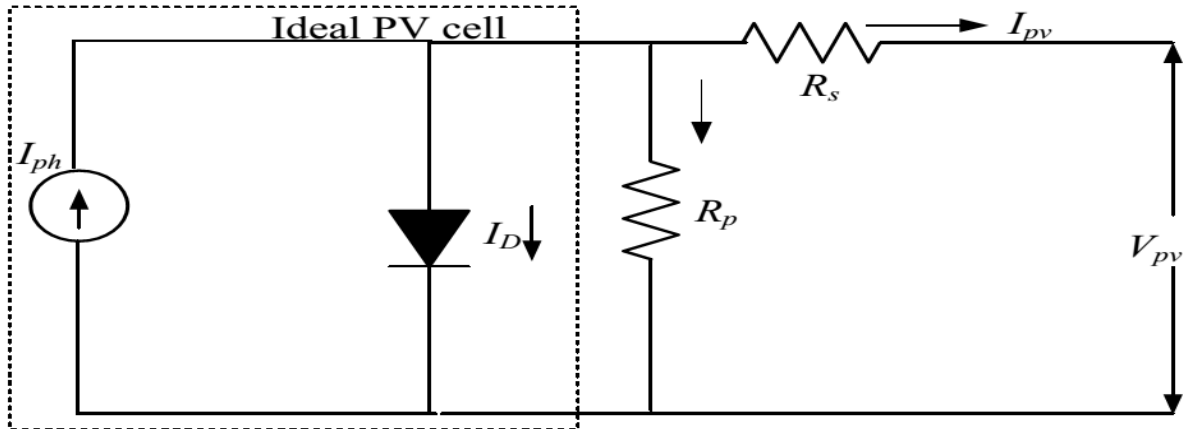


Figure.2: An analogous PV cell circuit with a single diode configuration

The model with a single diode is the simplest approach, which involves connecting a parallel connection between a diode and a current source. The quantity of light that strikes the cell is exactly proportional to the current source's output. The I-V curve may be fully described by this model with just three parameters: The open circuit voltage V_{oc} , short-circuit current I_{sc} , and diode ideality factor. A single diode model falls short of accurately capturing how the cell behaves in different environmental circumstances, particularly at low voltage. One series resistance R_s is added to this model to make it better. The model is the most used model for simulating PV systems because of its ease of use and high computational efficiency.

Applying Kirchhoff's current law, the mathematical formula of an actual PV cell is as follows.

$$I = I_{pv} - I_0 \left[\exp\left(\frac{V + R_s I}{\alpha V_T}\right) - 1 \right] - \frac{V + R_s I}{R_p} \tag{3}$$

Here,

$$V_T = \frac{V_s K T}{c} \tag{4}$$

$$I_{pv} = (I_{pv,n} + K_1 \Delta_t) \frac{r}{r_n}$$

$$I_0 = \frac{I_{sc} + K_t \Delta_t}{\exp\left[\frac{(V_{oc,n} + K_v \Delta_t)}{\alpha V_T}\right] - 1} \tag{5}$$

This $I_{pv,n}$ represents the PV cell output current's nominal value. R_p and R_s stand for solar resistance both in parallel and series respectively represent the actual open circuit voltage as

well nominal current value, respectively and V_T represent the thermal voltage. $V_{oc,n}$ and $I_{sc,n}$ denotes the current coefficient and short circuit voltage respectively. r and r_n show the nominal irradiation as well as the device surface irradiation. Δ_t Shows the variation between the actual temperature and the usual temperature.

3.2) DC-DC Boost Converter

The PV array and the inverter are connected by a DC-DC boost converter, which provides the required DC voltage and keeps the load voltage constant [27]. The voltage input-output relationship for the continuous conduction mode is as follows:

$$\frac{V_o}{V_{in}} = \frac{1}{1-D} \tag{6}$$

The input V_{in} and output V_o voltages of the boost converter are shown here, along with the duty cycle D . The output exceeds the input voltage as it rises from 0 to 1. Figure 3 shows a DC-DC boost converter configuration with PV.

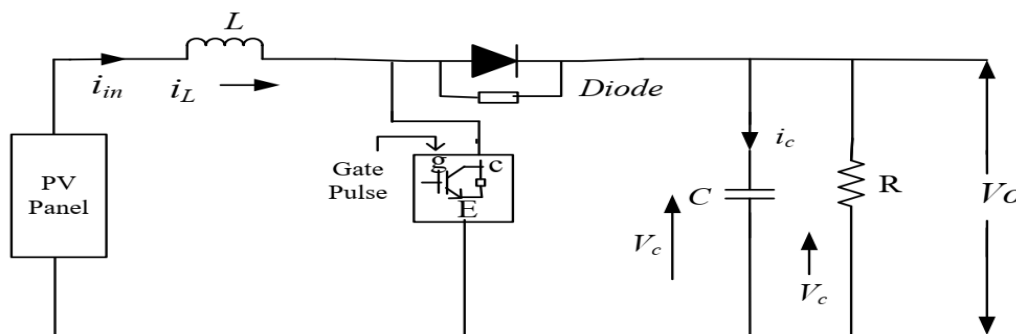


Figure.3: A structure of DC-DC boost converters with PV

In a solar array, the average current increases and the PV voltage lowers as the boost converter's duty cycle increases. As a result, when the duty cycle is increased, the PV array V-I characteristic's operational point moves to the left. In a similar vein, when the duty cycle decreases, The PV array's output voltage increases as the average current falls. As a result, the PV array V-I characteristic's operational point moves to the right. By automatically regulating the duty cycle of the DC-DC converter through P&O, a steady DC voltage is supplied at the RS-MLI terminal.

²⁷ Yatindra Gopal, et al., "Selected Harmonic Elimination for Cascaded Multilevel Inverter Based on Photovoltaic with Fuzzy Logic Control Maximum Power Point Tracking Technique", Technologies, Vol.6, No.62, 2018

3.3) P&O MPPT Technique

When a PV array is exposed to specific temperature and irradiance levels, To extract the maximum output power, the MPPT technology automatically calculates the voltage or current at which it should run. The P&O algorithm is widely used and appropriate for real-world scenarios. This algorithm's output is shown on the PV output screen. It is based on system disruption brought on by a falling or increasing duty cycle. A tiny amount of disturbance to the PV module's operating voltage causes a change in power, which is seen. An operational point is said to be approaching the MPP if there is a positive change in power. If there is a negative power change, The MPP is moved away from the operating point [28]. Consequently, in the subsequent perturbation cycle, the opposite perturbation direction is required. Duty cycle is produced throughout the repeated process and sent into the DC-DC boost converter. This technique works particularly well in settings where the air is steady or varies slowly. Nonetheless, by lowering the operating voltage response time, the P&O algorithm helps to minimize power loss inside the PV system.

3.4) Configuration of RSS-MLI

While a conventional inverter generates only two levels, multilevel inverters generate many levels. To create a single high-voltage switch, There is no series connection between the semiconductor devices.. In the output voltage waveform, Each device group contributes to a step. To get a nearly sinusoidal waveform, the steps are increased. With each level climb, the quantity of switches involved grows. Different voltage sources acquired from the capacitor voltage sources are often used to generate the multilevel inverter's output waveform. Here, a seven-level MLI is suggested, which has fewer switches than other well-known topologies. Because to the switch decrease, the initial cost is lowered. The initial cost will be lower with the suggested topology since only one switch needs to be added for every level increase. Seven MOSFET switches and three independent DC sources with a load make up the suggested MLI. There are seven levels of output voltage that can be obtained by switching the MOSFETS at the proper firing angles. Because MOSFETs switch quickly, they are recommended [29]. Reduced initial cost, better control, reduced losses from the removal of harmonics, and decreased total weight from using fewer components are all results of the decreased number of switches.

For many output levels that are less expensive and require fewer switching parts, RS-MLI is employed in this study. By protecting the switches from overvoltage and dV/dt breakdown consideration, the voltage stress on the switches is reduced by the suggested RS-MLI circuit.

²⁸ Gokhan YUKSEK et al., Gazi University Journal of Science, Vol.36, No.2, pp.608-622, 2023

²⁹ Uthirasamy, R, et al., 'Investigation on Three-Phase Seven-Level Cascaded DC-Link Converter Using Carrier Level Shifted Modulation Schemes for Solar PV System Applications', IET Renewable Power Generation, vol. 12, no. 04, pp. 439-449.

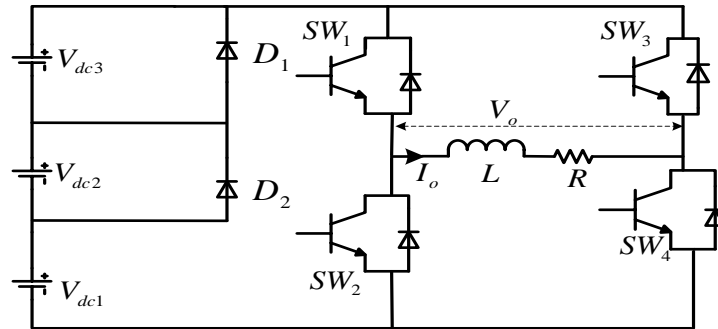


Figure.4: The suggested seven-level structure of RS-MLI

Figure 4 depicts the suggested configuration of the 7-level RS-MLI.

3.4.1) Modes of Operations

In four switches configured in an RS-MLI configuration $SW_1 - SW_4$ with two diodes (D_1 and D_2) are used. H-bridge switches, sometimes referred to as switches for function at a high switching frequency for polarity generation, while level generation switches operate at a lower frequency. As a result, it makes economic sense to use components with the H-bridge requires low switching power, while level generation requires high switching power [30]. The instances that follow give an overview of the RS-MLI working theory.

Case a: In the first scenario, current flows via the switches SW_1 and SW_2 , and diode D_1 and D_2 . At the output, across the load, the voltage is $+V_{dc1}$. Consequently, the output voltage across the load is $-V_{dc1}$ when SW_3 and SW_4 are activated.

Case b: In this instance, current passes via the diode D_2 and switches SW_1 and SW_2 . At the output, the voltage across the load is $V_{dc1} + V_{dc2}$. Consequently, during SW_3 and SW_4 switch activate, across the load the output voltage is equal to $-(V_{dc1} + V_{dc2})$.

Case c: Current flows through SW_1 and SW_2 in this manner. At the output, the voltage across the load is $V_{dc1} + V_{dc2} + V_{dc3}$, D_1 and D_2 reverse biased. Correspondingly when SW_3 and SW_4 are turned on, the output voltage is $-(V_{dc1} + V_{dc2} + V_{dc3})$.

Case d: This mode allows each SW_1 and SW_2 or SW_2 and SW_4 are ON, across the load, produces zero output voltage.

³⁰ Gunasekaran, R et al., International Journal of Microprocessors and Microsystems, pp.1-9, Vol.74, 2020

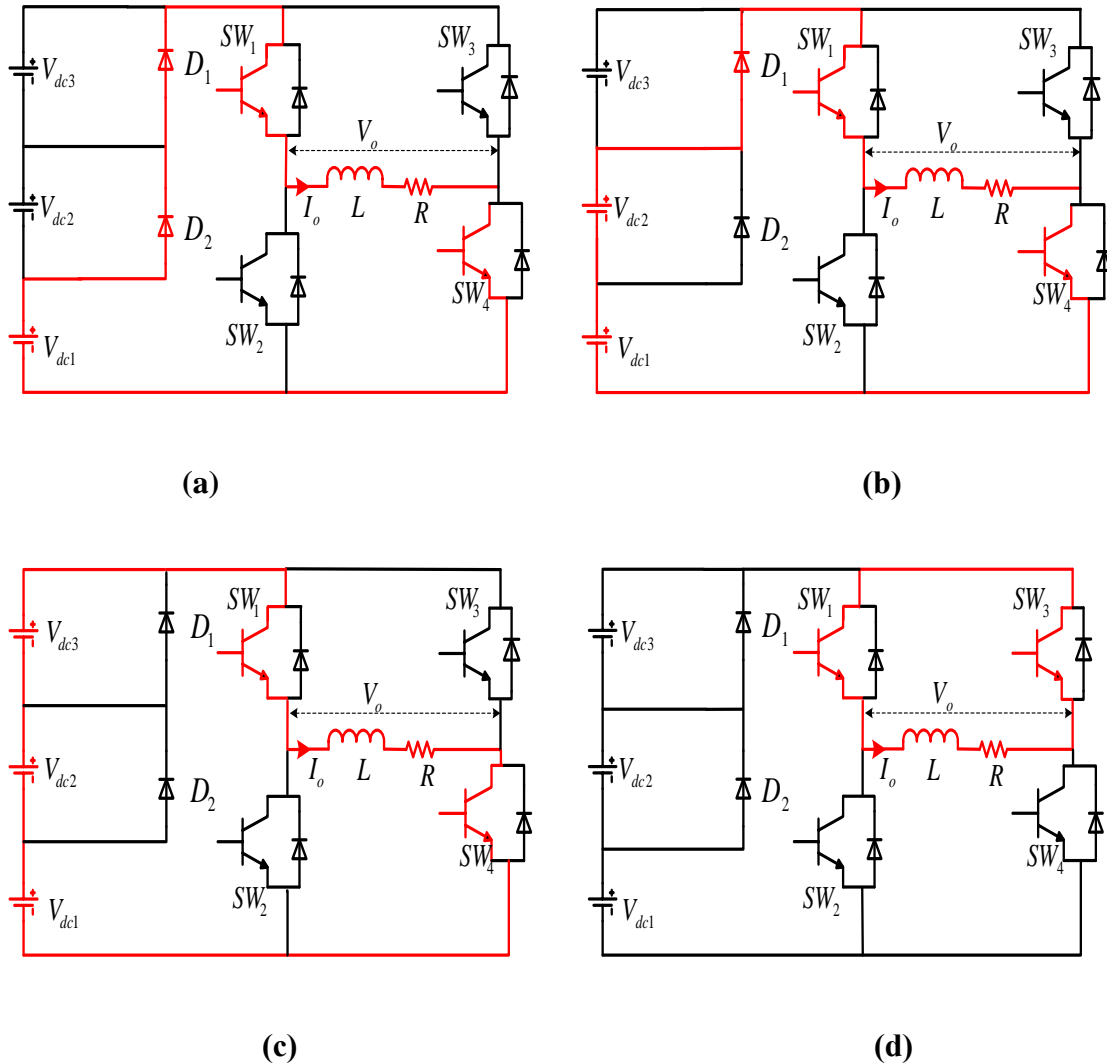


Figure.5: The configuration RSMLI is suggested to produce various voltage output values. (a) Instance a: + Vdc, (b) Instance b: 2Vdc, (c) Instance c: 3Vdc, (d) Instance d: 0

Figure 5 illustrates how the suggested RS-MLI generates various output voltage levels.

3.5) Harmonic elimination theory

Fourier analysis of the voltage produced by the multilayer inverter yields the expression for the multilayer voltage. The following describes the basic switching frequency management method when the DC input voltage of the multilayer inverter is equal:

$$V(t) = \sum_{n=1,3,5}^{\infty} \left(\frac{4V_{dc}}{n\pi} \right) \{ \cos n\theta_1 + \cos n\theta_2 + \dots, \cos n\theta_s \} \sin n\omega t \tag{7}$$

The PV module of the inverter's DC supply voltage V_{dc} , the switching angle θ , and the total number of switching angles s are shown here. The equation shows that the inverter does not

have even order harmonics since its output voltage is odd quarter-wave symmetric [31]. The odd order harmonics peak value θ_1, θ_2 , etc., is expressed using the device switching angle. The transcendental equation is the harmonics equation for the inverter voltage. Harmonics are eliminated using the n^{th} harmonic elimination theory, which can be expressed as follows.

$$\cos n\theta_1 + \cos n\theta_2 + \dots + \cos n\theta_s = 0 \tag{8}$$

3.6) Switching angle analysis

The SHE techniques are employed to acquire the seven levels of the output voltage. The harmonics of odd order can be avoided or eliminated by picking the suitable switching angle. The SHE techniques not only minimize overall harmonic distortion but also generate the necessary switching angle to give output voltage [32]. It also reduces electromagnetic interference and loss caused by higher frequency switching. In order to lower the output voltages THD, the critical switching angles $\theta_1, \theta_2, \dots, \theta_s$, are determined with respect to the required ideal reference voltage V . The Fourier coefficients' magnitude in relation is expressed as the reference voltage follows after normalization:

$$V = \left(\frac{4V_{dc}}{\pi} \right) \{ \cos\theta_1, \cos\theta_2, \dots, \cos\theta_s \} \tag{9}$$

3.7) FOPID controller

The differential equation for a fractional order PID controller is written as,

$$u(t) = k_p e(t) + k_i D_t^{-\lambda} e(t) + k_d D_t^\mu e(t) \tag{10}$$

Once the FOPID has been determined applying the Laplace transform, the function of continuous transfer is

$$G_c(s) = k_p + k_i s^{-\lambda} + k_d s^\mu \tag{11}$$

The design of three parameters is required while creating a FOPID controller k_p, k_i, k_d as well as two parameters λ, μ that are not usually represented as integers.

³¹ M. H. Yabalar et al., IEEE Access, vol. 12, pp. 71010-71023, 2024

³² Yasin Bektas, et al., "Red deer algorithm-based selective harmonic elimination technique for multilevel inverters", Bulletin of Electrical Engineering and Informatics, Vol. 12, No. 5, 2023, pp. 2643-2650

3.8) SBOA utilized FOPID gain parameters optimization

Secretary birds' natural environment provides a means of survival that serves as the model for a unique population-based metaheuristic algorithm dubbed SBOA, which is presented in this work. For secretary birds to survive, they must constantly forage for food and avoid being chased by predators. The data is essential in the development of a novel metaheuristic algorithm that leverages secretary bird survival skills to tackle practical optimization issues. The exploitation stage of the algorithm mimics secretary birds fleeing from predators, while the exploration phase replicates the bird's hunting snakes [34]. Secretary birds study their surroundings and select the best route to a haven at this stage of development. The ideal solution to the optimization problem is found by repeatedly going through these two phases, subject to termination requirements.

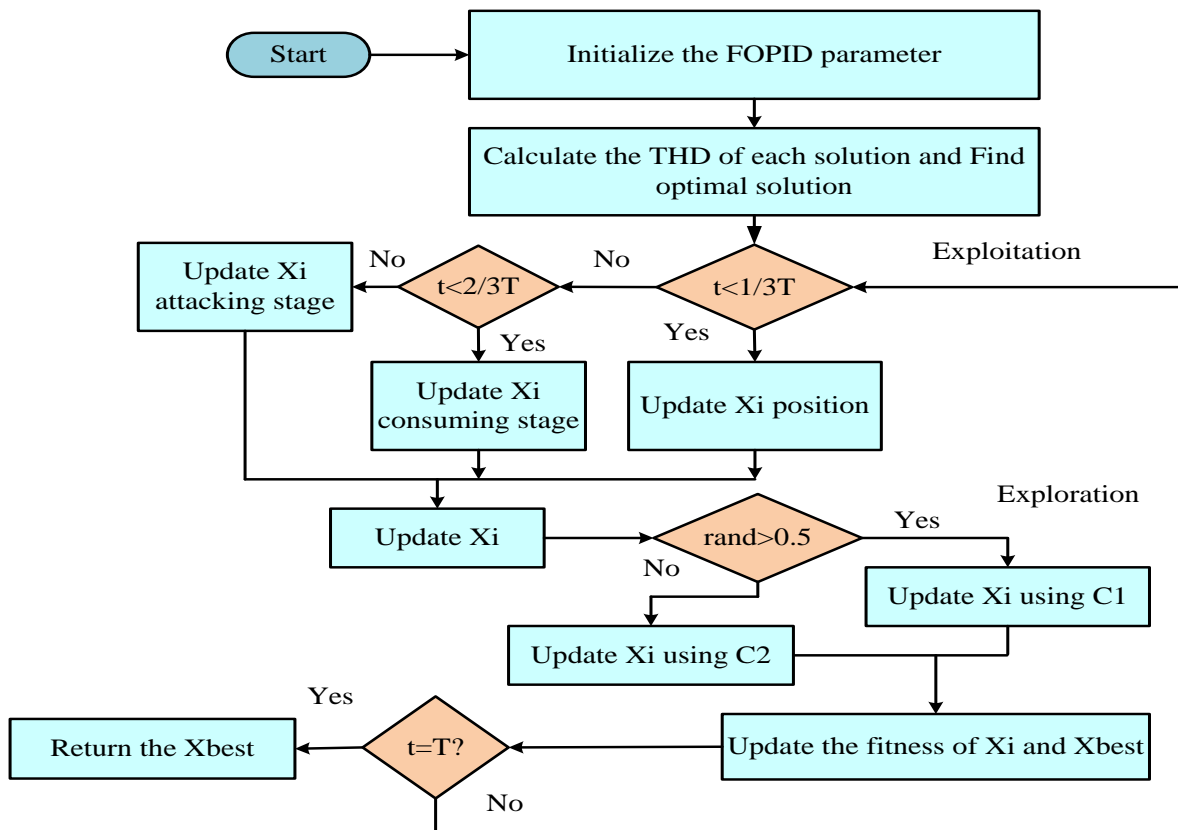


Figure.6: Flow diagram of the proposed SBOA

This section contains a behavioural mathematical model of the secretary bird as well as an explanation of the proposed SBOA. Figure 6 displays the planned SBOA's flow diagram.

³⁴ Youfa Fu, Dan Liu, Jiadui Chen and Ling He, "Secretary bird optimization algorithm: a new metaheuristic for solving global optimization problems".

3.9) Mathematical modelling of the SBOA

This subsection presents the SBOA mathematical model for optimizing the FOPID gain settings.

3.9.1) Initial preparation phase

The search space's gain parameters are initialized at random points in the first implementation of the SBOA.

$$X_{ij} = lb_j + r(ub_j - lb_j), i = 1, 2, \dots, N, j = 1, 2, \dots, Dim \tag{12}$$

Here, X_i shows the actual position among the i^{th} gain parameter and r stands for an arbitrary number in the range of 0 to 1, where lb_j and ub_j stands for the lower and upper bounds, respectively.

Candidate solution population functions as the starting point for optimization in the SBOA population-based approach. These potential answers are produced at random within the problem's upper and lower bound constraints. With each iteration, the finest option is generally regarded as the one that has been discovered thus far.

$$X = \begin{bmatrix} x_{1,1} & x_{1,2} & \dots & x_{1,j} & \dots & x_{1,Dim} \\ x_{2,1} & x_{2,2} & \dots & x_{2,j} & \dots & x_{2,Dim} \\ \vdots & \vdots & \ddots & \vdots & \ddots & \vdots \\ x_{i,1} & x_{i,2} & \dots & x_{i,j} & \dots & x_{i,Dim} \\ \vdots & \vdots & \ddots & \vdots & \ddots & \vdots \\ x_{N,1} & x_{N,2} & \dots & x_{N,j} & \dots & x_{N,Dim} \end{bmatrix}_{N \times Dim} \tag{13}$$

Here, X said gain parameter collective, X_i stated the i^{th} gain parameter, X_{ij} said the i^{th} gain parameter j^{th} variable value, N represents the sum of the parameter group, along with Dim represents the size of concern variable.

Every one parameter represents a possible solution to maximize the values, and the objective function can thus be evaluated using the values for the problem variables that each gain parameter suggests. After that, a vector is created by compiling the objective function's values.

$$F = \begin{bmatrix} F_1 \\ \vdots \\ F_i \\ \vdots \\ F_N \end{bmatrix}_{N \times 1} = \begin{bmatrix} F(X_1) \\ \vdots \\ F(X_i) \\ \vdots \\ F(X_N) \end{bmatrix}_{N \times 1} \tag{14}$$

Here, F indicates how objective values work. Additionally, the vector displays the F_i objective function's true value that the i^{th} gain parameter achieved. To keep the SBOA members informed, two different secretary bird natural actions as hunting and fleeing have been used. Every member of the gain parameters colony is thus changed twice throughout with each iteration.

3.9.2) Hunting tactics (period of exploration)

The three main stages of secretary bird hunting are searching for prey, consuming prey, and attacking prey. Based on biological statistics of the stages and durations of each phase, it has divided the hunting technique of the secretary bird into three separate time frames, namely $t < \frac{1}{3}T, \frac{1}{3}T < t < \frac{2}{3}T$ and $\frac{2}{3}T < t < T$ the three equivalent phases. Thus, each SBOA phase is represented as:

Stage 1 (Prey Searching): Typically, Secretary birds search for potential prey, especially snakes, during the beginning of the hunting season.

$$\text{While } t < \frac{1}{3}T, x_{i,j}^{newP1} = x_{i,j} + (x_{ran-1} - x_{ran-2})R_1 \tag{15}$$

$$X_i = \begin{cases} X_i^{new,P1}, & \text{if } F_i^{new,P1} < F_i \\ X_i, & \text{else} \end{cases} \tag{16}$$

Stage 2 (Consumption Prey): After locating a snake, a secretary bird employs a special hunting strategy. Where the Secretary Bird is in the Prey Consumption Stage is altered.

$$\text{While } \frac{1}{3}T < t < \frac{2}{3}T, x_{i,j}^{newP1} = x_{best} + \exp((t/T) \wedge 4) \times (RB - 0.5) \times (x_{best} - x_{i,j}) \tag{17}$$

Here, x_{best} denotes the current best value and $randn(1, Dim)$ is an array of dimensions $1 \times Dim$ created at random from a typical normal distribution (mean 0, standard deviation 1).

Stage 3 (Attacking Prey): Typically, the secretary bird kicks its legs at this time, swiftly lifting its leg and delivering precise kicks using its sharp claws, often aiming for the head of

the snake. During the Attacking Prey phase, the secretary bird's location is updated.

$$\text{While } t > \frac{2}{3}T, x_{i,j}^{new P1} = x_{best} + \left(\left(1 - \frac{t}{T} \right) \wedge \left(2 \times \frac{t}{T} \right) \right) \times x_{i,j} \times RL \tag{18}$$

3.9.3. Escape strategy (exploitation stage)

Two primary categories can be used to roughly classify these tactics. The initial strategy is fighting or speeding. Especially long legs allow secretary birds to run at incredibly high speeds. Both evasion strategies employed by secretary birds.

$$x_{i,j}^{new P2} = \begin{cases} C_1 : x_{best} + (2RB - 1) \left(1 - \frac{t}{T} \right)^2 x_{i,j}; & \text{if } r \text{ and } < r_i \\ C_2 : x_{i,j} + R_2 (x_{rand} - K \times x_{i,j}); & \text{else} \end{cases} \tag{19}.$$

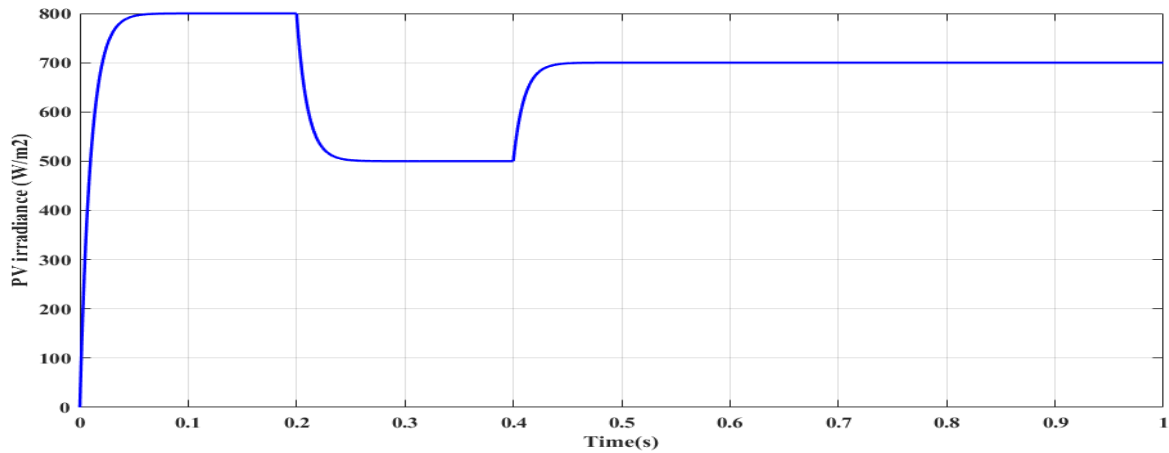
4) Simulation Outcomes And Discussions

The performance of the recommended methodology is implemented and verified in this part. The MATLAB/Simulink platform can be used to accomplish the suggested approach. The reduction of THD and the effectiveness of the suggested controller that is employed to support PV applications that are integrated into the grid, validate the predicted technique. The FOPID controller with SBOA optimization for RS- THD based on MLI reduction is included in the suggested system. Table 1 lists the PV implementation parameters.

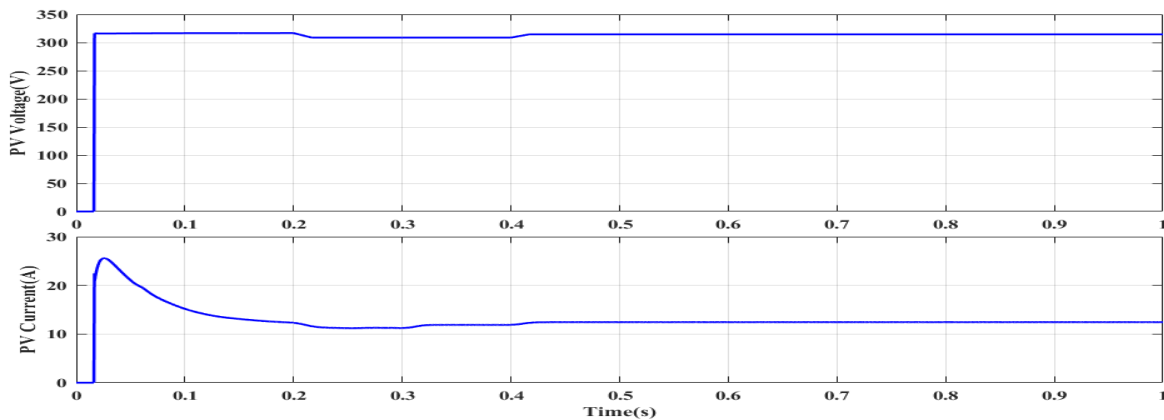
Table 1: PV implementation specifications

| <i>Specifications</i> | <i>Values</i> |
|-----------------------|---------------|
| Ncell | 96 |
| Voc (V) | 64.2 |
| Isc (A) | 5.96 |
| Vmp (V) | 54.7 |
| Imp (A) | 5.58 |
| IL (A) | 6.0092 |
| I0 (A) | 6.30e-12 |
| Diode ideality factor | 0.94504 |

| | |
|------------|----------|
| Rsh (ohms) | 269.5934 |
| Rs (ohms) | 0.37152 |
| fn (Hz) | 60 |



(a)



(b)

Figure.7: The investigation of (a) PV irradiance, (b) Voltage and Current

Figure 7 shows the PV's irradiance input, which aids in producing the most power possible and is enhanced by using a DC-DC converter, as well as the corresponding current and voltage that are produced. Figure 8 depicts the DC-link voltage performance study. Figure 9 presents the load voltage and current performance analysis.

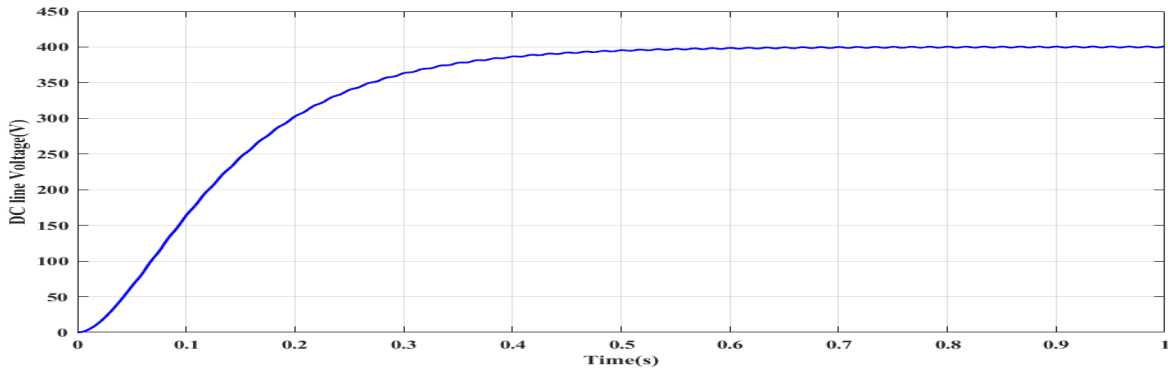


Figure.8: The performance study of DC link voltage

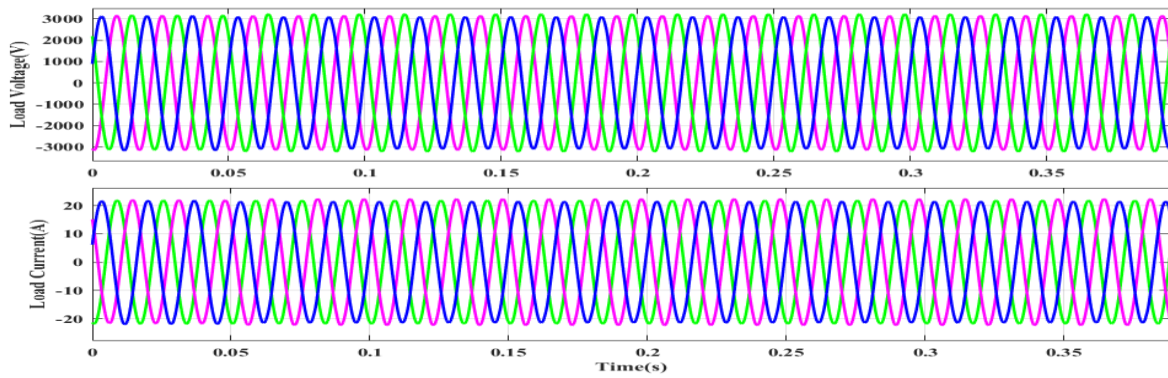


Figure.9 : The load voltage and current performance analysis

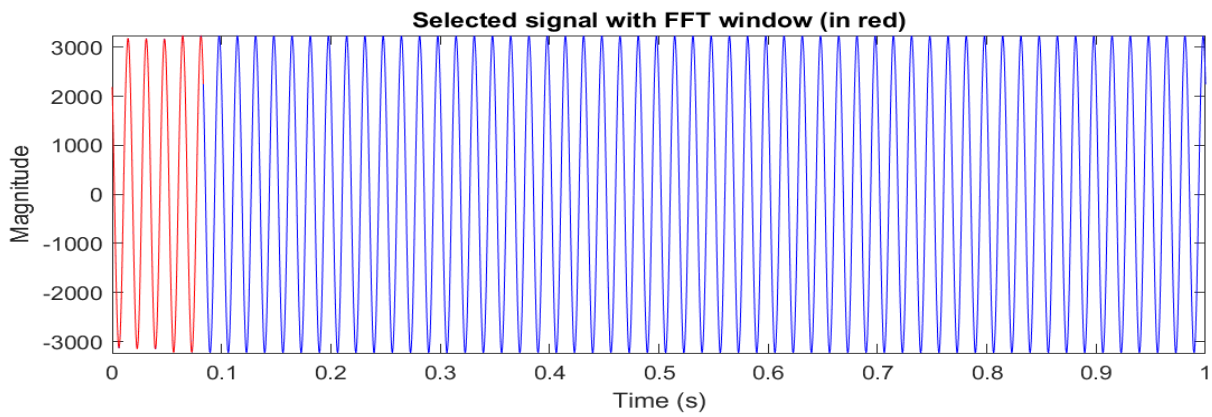
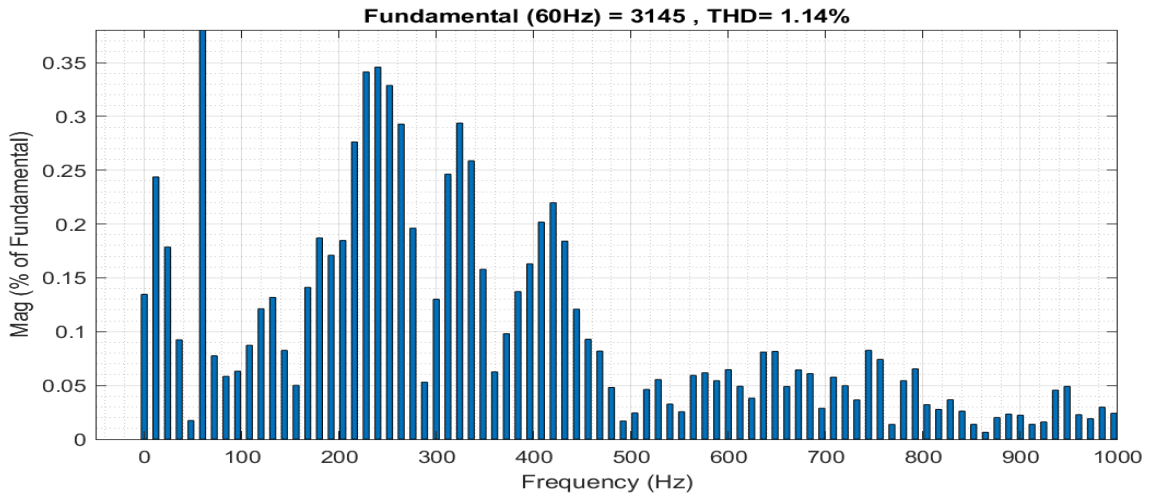
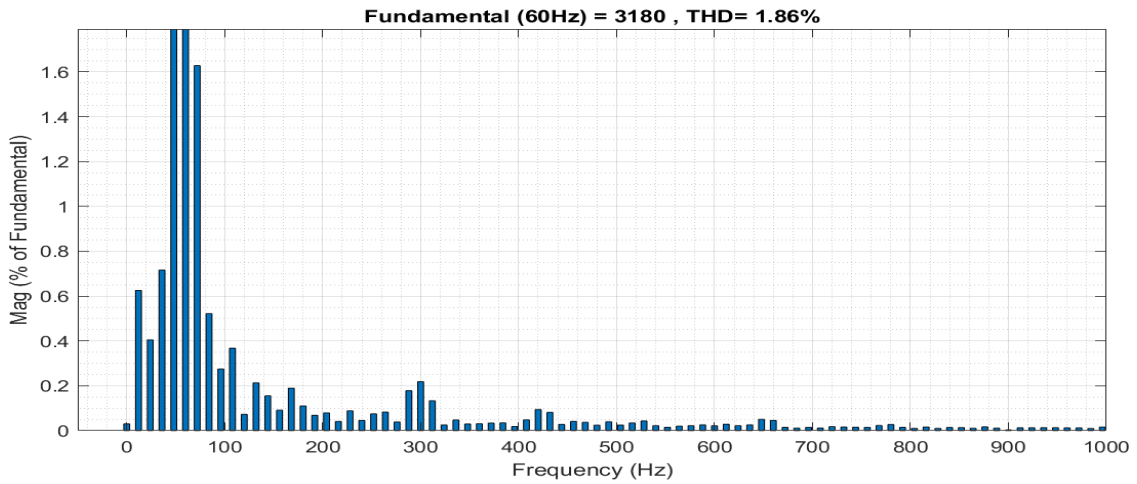


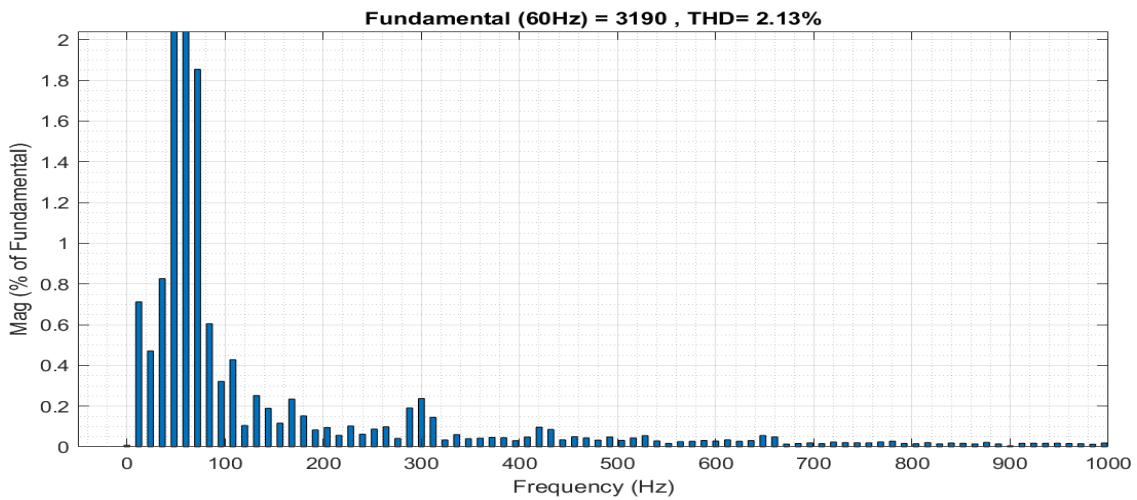
Figure.10: output voltage waveform of SBOA-FOPID controller



(a)



(b)



(c)

Figure.11: The FFT analysis of (a) WSOA-FOPID, (b) WSOA-PID and (c) GA-PID

To reduce the THD, It is advised to use a greater controller gain setting than the conventional PID controller gain values. Figure 10 demonstrates the SBOA's FFT analysis for the recommended controller. In the proposed system, the grid side voltage THD analysis was compared with several methods, such as WSOA-FOPID, WSOA-PID, and GA-PID. This study demonstrates that the harmonics have significantly decreased. Additionally, it is desirable to reduce voltage THD in several circumstances. The harmonic analysis of the load voltage using a few previous research projects is displayed in Figure 11. The comparison analysis based on this consideration shows how effective the suggested controller is with respect to the assessment parameters. The THD comparative analysis shows that the recommended strategy successfully lowers THD more than other conventional methods.

5) Conclusion

Thus, for a grid-connected, three-phase PV system, this research proposed an SBOA optimized FOPID controller in a seven level RSMLI. With the aid of the SBOA, System performance was enhanced by adjusting the FOPID controller's gain parameter. The PV system linked to the grid's power characteristics were regulated by considering the suggested technique. The MATLAB/Simulink was used in the implementation of the suggested approach. and its performances were assessed and contrasted with those of a few current controllers, including the WSOA-FOPID, GA-PID, and WSOA-PID controllers. This method is put into practice by determining the THD analysis at various time instants and evaluating its performance. Two primary controllers are used in the suggested system. The P&O MPPT controller of the DC/DC boost converter monitors the PV panels' maximum power output. Both the output performance and the THD were improved by adjusting the inverter control signals. Reducing the THD improved the grid-connected PV array's performance, according to the FFT analysis and simulation results. Thus, the focus of this paper is on decreased switch In-depth discussions are held regarding THD analysis for various approaches and modified MLI topologies. This paper's major goal is to discuss reduced switch and reduce THD that have been implemented successfully.